To appear in *Molecular Physics*
Vol. 00, No. 00, Month 200x, 1–17

RESEARCH ARTICLE

On the relation between thermostatted ring polymer molecular dynamics and exact quantum dynamics

Timothy J. H. Hele

(*Received 00 Month 200x; final version received 00 Month 200x*)

Here we obtain the explicit difference in the propagator between Thermostatted Ring Polymer Molecular Dynamics (TRPMD) and Matsubara dynamics, a recently-derived form of linearization which conserves the quantum Boltzmann distribution. Examination of this approximation leads to the new results that the TRPMD force on the centroid is identical to the Matsubara force on the centroid, and that (in a harmonic potential) the friction matrix can be chosen to produce either the correct oscillation frequency of the higher ring-polymer normal modes or the correct maximum in their position spectrum. This is illustrated with the position-squared autocorrelation function where TRPMD improves upon other similar methods. However, no physical choice of friction resolves qualitatively incorrect fluctuation dynamics at barriers. These results are broadly consistent with previous numerical studies and advise the use of TRPMD for spectra.

Keywords: Quantum dynamics, correlation function, path integral, ring polymer, Langevin dynamics

1. Introduction

The computation of thermal time-correlation functions is of central importance in chemical physics [1, 2] in order to evaluate many physically observable quantities such as reaction rates, diffusion constants, spectra and scattering data. [3, 4]

Exact evaluation of the quantum correlation function scales exponentially with system size and so is impractical for more than a few atoms. [3] There is consequently a need for computationally tractable approximations to quantum time-correlation functions [4, 5], preferably which are known to be equivalent to the quantum result in certain limits, and for which the likely error is known in advance of calculation.

Since a purely classical calculation neglects zero-point energy and tunnelling effects, various approximate methods have been developed which combine quantum Boltzmann statistics with classical mechanics, including the linearized semiclassical initial value representation (LSC-IVR) [4, 6–8], Centroid Molecular Dynamics (CMD) [9–16], and Ring Polymer Molecular Dynamics (RPMD) [3, 17–19].

Recently, Thermostatted Ring Polymer Molecular Dynamics (TRPMD) has been introduced, which applied a Langevin thermostat [20–22] to the dynamics of the ring polymer [23–25], and which accurately replicated multidimensional spectra where CMD and RPMD fail [26, 27] and correctly predicted the diffusion and rotational constants of liquid water [24, 25]. However, in numerical tests TRPMD did not generally improve upon RPMD for reaction rate calculation [28].

Very recently, both RPMD and CMD have been obtained from the exact quantum time-correlation function via “Matsubara dynamics”, a form of linearization

---

Corresponding author: tjhh2@cam.ac.uk
Department of Chemistry, University of Cambridge, Lensfield Road, Cambridge, CB2 1EW, UK,
Baker Laboratory, Cornell University, 259 East Avenue, Ithaca, NY 14850, USA.

ISSN: 0040-5167 print/ISSN 1754-2278 online

DOI: 10.1080/0040516YYxxxxxxxx
http://www.informaworld.com

which conserves the quantum Boltzmann distribution [29, 30]. However, Matsubara dynamics is not amenable to computation in large systems since it suffers from the sign problem due to a phase factor in the complex quantum Boltzmann distribution [30]. An approximation to Matsubara dynamics where the centroid moves in the mean field of the other Matsubara modes leads to CMD, and by moving the momentum contour in the quantum Boltzmann distribution and discarding the imaginary Liouvillian which results, RPMD arises [30].

This motivates finding whether there are other approximations to Matsubara dynamics which also preserve some of its appealing features, but are more accurate for certain systems than RPMD or CMD.

In this paper we obtain the explicit error term between the TRPMD Fokker-Planck operator and the Matsubara dynamics Liouvillian and show that this does not act on the centroid. In an appendix we clarify the analytic continuation in the Matsubara momenta by showing that the region of the complex plane through which the contour is moved is holomorphic (free from poles). We also show that one choice of the friction matrix causes all higher normal modes oscillate at the correct (external) frequency in a harmonic potential, and a different value of the friction matrix is required to produce the correct (physical) peak in the autocorrelation spectrum.

This is illustrated with the position-squared autocorrelation function, where TRPMD has the correct zero-time value and (with a particular choice of friction) the correct frequency; neither RPMD nor CMD can reproduce both these properties [31, 32]. We then examine a parabolic barrier and find that application of any meaningful (i.e. positive) friction does not cause the erroneously bound normal modes in TRPMD to become scattering, and nor does it cause unbound modes to have the correct escape frequency, meaning that application of friction is unlikely to assist in the accuracy of reaction rate or diffusion calculation.

We begin with a brief review of Matsubara dynamics and its relationship to RPMD and CMD in section 2, where we then place TRPMD in the context of Matsubara dynamics and give the error in the propagator between the two methods. We examine various choices of the friction matrix in section 3, and present a some numerical examples in 4 before discussion in section 5 and conclusions in section 6.

2. Theory

For simplicity, we consider a one-dimensional system with mass m, co-ordinate q, and Hamiltonian $\hat{H} = \hat{p}^2/2m + V(\hat{q})$, where $V(q)$ is the potential.[1] We assume familiarity with Ref. [29] which derives Matsubara dynamics from the exact quantum Kubo [33] expression, and here review the movement of the momentum contour in the complex plane [30] in order to obtain the analytically-continued Matsubara propagator [Eq. (6)] which we then relate to TRPMD.

The classical-like Matsubara correlation function is

$$C_{AB}^{[M]}(t) = \frac{\alpha_M}{2\pi\hbar} \int d\mathbf{P} \int d\mathbf{Q}\ e^{-\beta[H_M(\mathbf{P},\mathbf{Q}) - i\theta_M(\mathbf{P},\mathbf{Q})]} A(\mathbf{Q}) e^{\mathcal{L}_{\mathrm{Mat}}^{[M]} t} B(\mathbf{Q}) \tag{1}$$

---

[1] Extensions to further dimensions follows immediately and merely requires more indices. Here we consider dynamics on a single Born-Oppenheimer potential energy surface and at temperatures sufficiently high that Bose-Einstein and Fermi-Dirac statistics need not be considered, which is the case for most systems to which CMD, RPMD and TRPMD have been applied.

where $(\mathbf{P},\mathbf{Q})$ are ring polymer normal modes [23, 29, 34], $\beta \equiv 1/k_\mathrm{B}T$, $A(\mathbf{q}) = \frac{1}{N}\sum_{i=0}^{N-1} A(q_i)$ and likewise for $B(\mathbf{Q})$. The Matsubara Hamiltonian is

$$H_M(\mathbf{P},\mathbf{Q}) = \sum_{j=-(M-1)/2}^{(M-1)/2} \frac{P_j^2}{2m} + U^{[M]}(\mathbf{Q}), \tag{2}$$

$U^{[M]}(\mathbf{Q})$ is the potential defined in Ref. [29], $\alpha_M = \hbar^{M-1}[(M-1)/2]!^2$, and the phase factor is

$$\theta_M(\mathbf{P},\mathbf{Q}) = \sum_{j=-(M-1)/2}^{(M-1)/2} P_j \tilde{\omega}_j Q_{-j} \tag{3}$$

where $\tilde{\omega}_j = 2\pi j/\beta\hbar$ are the Matsubara frequencies [35] which, in this definition, can be negative. The integrals are taken to mean $\int d\mathbf{P} = \prod_{j=-(M-1)/2}^{(M-1)/2} \int_{-\infty}^{\infty} dP_j$ and likewise for $\int d\mathbf{Q}$. Matsubara dynamics is defined by the Liouvillian

$$\mathcal{L}_\mathrm{Mat}^{[M]} = \frac{\mathbf{P}}{m}\overrightarrow{\nabla}_\mathbf{Q} - U^{[M]}(\mathbf{Q})\overleftarrow{\nabla}_\mathbf{Q} \cdot \overrightarrow{\nabla}_\mathbf{P} \tag{4}$$

such that $\mathcal{L}_\mathrm{Mat}^{[M]} \equiv \{\cdot, H_M(\mathbf{P},\mathbf{Q})\}$ where $\{\cdot,\cdot\}$ is the classical Poisson bracket. [21]

The Matsubara correlation function in Eq. (1) suffers from the sign problem, such that it is not amenable to computation in complex systems. To make the distribution real, we continue into the complex plane of $\mathbf{P}$ with

$$\bar{P}_j = P_j - im\tilde{\omega}_j Q_{-j} \tag{5}$$

for all j (such that no analytic continuation is necessary for the momentum centroid) to give

$$\mathcal{L}_{\bar{\mathbf{P}}}^{[M]} = \mathcal{L}_\mathrm{RP}^{[M]} + i\mathcal{L}_\Im^{[M]} \tag{6}$$

where $\mathcal{L}_\mathrm{RP}^{[M]}$ is the ring polymer Liouvillian,

$$\mathcal{L}_\mathrm{RP}^{[M]} = \sum_{j=-(M-1)/2}^{(M-1)/2} \frac{\bar{P}_j}{m}\frac{\partial}{\partial Q_j} - \left[\frac{\partial U^{[M]}(\mathbf{Q})}{\partial Q_j} + m\tilde{\omega}_j^2 Q_j\right]\frac{\partial}{\partial \bar{P}_j} \tag{7}$$

and the imaginary component of the Liouvillian is

$$\mathcal{L}_\Im^{[M]} = \sum_{j=-(M-1)/2}^{(M-1)/2} \tilde{\omega}_j \left(\bar{P}_j \frac{\partial}{\partial \bar{P}_{-j}} - Q_j \frac{\partial}{\partial Q_{-j}}\right), \tag{8}$$

which does not act directly upon the centroid since $\omega_0 = 0$. This transformation also converts the complex Matsubara distribution into the real ring polymer distribution,

$$e^{-\beta[H_M(\mathbf{P},\mathbf{Q}) - i\theta_M(\mathbf{P},\mathbf{Q})]} = e^{-\beta R_M(\bar{\mathbf{P}},\mathbf{Q})} \tag{9}$$

where the ring-polymer Hamiltonian is

$$R_M(\bar{\mathbf{P}},\mathbf{Q}) = \sum_{j=-(M-1)/2}^{(M-1)/2} \left(\frac{\bar{P}_j^2}{2m} + \tfrac{1}{2} m \tilde{\omega}_j^2 Q_j^2 \right) + U^{[M]}(\mathbf{Q}). \tag{10}$$

Both $\mathcal{L}_{\mathrm{RP}}^{[M]}$ and $\mathcal{L}_{\Im}^{[M]}$ independently conserve the quantum Boltzmann distribution.

In Ref [30], it was unknown whether the complex plane in $\mathbf{P}$ was holomorphic and the authors proposed following a path in the complex plane while gradually discarding $\mathcal{L}_{\Im}^{[M]}$ en route in order to keep the dynamics real, thereby moving smoothly from Matsubara dynamics to RPMD. In Appendix A, we place the analytic continuation on a stronger theoretical footing by proving that the complex dynamics generated by $\mathcal{L}_{\bar{\mathbf{P}}}^{[M]}$ is analytic (free from singularities) everywhere in the complex plane of $\mathbf{P}$, such that the Matsubara correlation function Eq. (1) is rigorously equal to

$$C_{AB}^{[M]}(t) = \frac{\alpha_M}{2\pi\hbar} \int d\bar{\mathbf{P}} \int d\mathbf{Q}\; e^{-\beta R_M(\bar{\mathbf{P}},\mathbf{Q})} A(\mathbf{Q}) e^{\mathcal{L}_{\bar{\mathbf{P}}}^{[M]} t} B(\mathbf{Q}) + \mathcal{E}(t) \tag{11}$$

where $\mathcal{E}(t)$ corresponds to the vertical edges of the integration contour; in Appendix A we give evidence to show that in many cases the edge term will vanish, though for an arbitrary system propagated to a finite time it is, strictly speaking, part of the error term between Matsubara dynamics and RPMD/TRPMD.

Although Eq. (11) contains the real ring polymer distribution, $i\mathcal{L}_{\Im}^{[M]}$ causes unstable complex trajectories [36, 37] which are no easier to treat numerically than the sign problem in the complex Matsubara distribution. [30]

This motivates finding computationally tractable approximations to Eq. (11); of course, one could arbitrary discard (or add) any term to the dynamics in $\mathcal{L}_{\mathrm{Mat}}^{[M]}$ to produce an approximate method, but in order to obtain a method which would be of practical use we impose the stringent requirements that the approximation leads to real trajectories, and that it conserves the Boltzmann distribution and obeys detailed balance. In addition, the resulting correlation function should preferably agree with Matsubara dynamics (and the exact quantum dynamics) up to a high order in time, and not make any direct alteration to the motion of the centroid.

In previous research [30] two approximate methods were found which satisfied most or all of the above criteria. Discarding $i\mathcal{L}_{\Im}^{[M]}$, in order to make the trajectories real but still conserve the quantum Boltzmann distribution, produces RPMD. However, discarding $i\mathcal{L}_{\Im}^{[M]}$ had the unpleasant side-effect of also raising the oscillation frequency of the higher ($j \neq 0$) normal modes; in a harmonic potential with external frequency ω_h they oscillate at $\bar{\omega}_j = \sqrt{\omega_h^2 + \tilde{\omega}_j^2}$. It was also shown that a mean-field approximation to Eq. (11) leads to CMD [30]. This research speculated that there may be other approximations to Matsubara dynamics that could (in some circumstances) be more accurate still [30].

This article considers whether it would be possible to obtain a dynamics which (in addition to all the criteria above) also has the correct oscillation frequency of the higher normal modes in a harmonic system (or produces the correct peak in the position-autocorrelation spectrum of each normal mode) and is therefore likely to improve upon RPMD and CMD in moderately harmonic systems where these oscillations are important, such as multidimensional spectra.[1]

---

[1] The higher normal modes are not explicitly represented in CMD, though are sometimes used as a com-

Addition of a friction (Langevin) term to the dynamics of a harmonic oscillator is known to decrease the oscillation frequency [1, 21] and so, instead of *discarding* the imaginary Liouvillian (giving RPMD), here we consider *replacing* it by a friction term. Mathematically, we therefore define an approximate dynamics with a Fokker-Planck operator

$$\mathcal{A}_{\mathrm{RP}}^{[M]\dagger} = \mathcal{L}_{\mathrm{RP}}^{[M]} + \mathcal{A}_{\mathrm{wn}}^{[M]\dagger} \tag{12}$$

where the white-noise thermostat which conserves the ring-polymer distribution $e^{-\beta R_M(\bar{\mathbf{P}},\mathbf{Q})}$ is

$$\mathcal{A}_{\mathrm{wn}}^{[M]\dagger} = -\bar{\mathbf{P}} \cdot \mathbf{\Gamma} \cdot \nabla_{\bar{\mathbf{P}}} + \frac{m}{\beta} \nabla_{\bar{\mathbf{P}}} \cdot \mathbf{\Gamma} \cdot \nabla_{\bar{\mathbf{P}}} \tag{13}$$

with $\mathbf{\Gamma}$ an $M \times M$ positive semidefinite friction matrix whose value is given in section 3.1. This allows us to approximate Eq. (11) as

$$C_{AB}^{[M]}(t) \simeq \frac{\alpha_M}{2\pi\hbar} \int d\bar{\mathbf{P}} \int d\mathbf{Q}\, e^{-\beta R_M(\bar{\mathbf{P}},\mathbf{Q})} A(\mathbf{Q}) e^{\mathcal{A}_{\mathrm{RP}}^{[M]\dagger} t} B(\mathbf{Q}), \tag{14}$$

which is TRPMD.[1]

Comparison of the propagators in Eqs. (11) and (12) leads to the new result that the TRPMD force on the centroid is equivalent to that in Matsubara dynamics,

$$\mathcal{L}_{\bar{\mathbf{P}}}^{[M]} \bar{P}_0 = \mathcal{A}_{\mathrm{RP}}^{[M]\dagger} \bar{P}_0 = -\frac{\partial U^{[M]}(\mathbf{Q})}{\partial Q_0} \tag{15}$$

so that the approximation from Matsubara dynamics to TRPMD does not directly affect the centroid motion, partly explaining the numerically-observed accuracy of TRPMD correlation functions of the ring polymer centroid [24, 25]. Previously TRPMD was obtained from RPMD by adding a friction term and without a motivation from quantum dynamics [24, 28]; here we give the error term between the quantum result and TRPMD: they are discarding the dynamics of the highest $(N - M)$ normal modes to give Matsubara dynamics (see Eq. (B2) of Ref. [29]), the edges of the contour used in analytic continuation (which we suspect to be zero, see Eq. (A10)), and the difference between the TRPMD and Matsubara propagators, namely $i\mathcal{L}_{\Im}^{[M]} - \mathcal{A}_{\mathrm{wn}}^{[M]\dagger}$.

3. Friction considerations

Since TRPMD can be related to Matsubara dynamics which, in turn, has a derivation from the exact quantum result, we seek to determine the optimal friction matrices which cause TRPMD to replicate specific features of Matusbara dynamics, namely (i) the correct (external) oscillation frequency of the higher normal modes in a harmonic potential, (ii) the correct maximum in the position spectra of each normal mode, and (iii) the correct barrier fluctuation dynamics.

---

putational device to construct the mean-field potential[38].

[1] Strictly speaking, this is TRPMD with Matsubara rather than ring-polymer frequencies, but will converge to conventional TRPMD in the limit of large M[30].

3.1. *Oscillation frequency*

We study the harmonic potential as a model bound system,

$$V(q) = \tfrac{1}{2} m\omega_h^2 q^2 \tag{16}$$

for which the ring polymer normal modes decouple and the dynamics can be solved exactly. For analytically continued Matsubara dynamics [Eq. (11)] in a harmonic potential, [30]

$$Q_j(t) = Q_j \cos(\omega_h t) + \frac{\bar{P}_j}{m\omega_h} \sin(\omega_h t) + i\frac{\tilde{\omega}_j}{\omega_h} Q_{-j} \sin(\omega_h t) \tag{17}$$

and all modes oscillate at the external frequency ω_h.

For TRPMD, the trajectories are not deterministic and we define the time-evolved phase-space density $\mathcal{Q}_j(t) \equiv \mathcal{Q}_j(Q_j, P_j, t)$ which is evolved with $\mathcal{A}_{\mathrm{RP}}^{[M]\dagger}$ from initial conditions of (Q_j, P_j) at $t = 0$. Exact solution for $\mathcal{Q}_j(t)$ leads to three regimes depending on the strength of the applied friction (as for a conventional damped harmonic oscillator); the underdamped, critically damped and overdamped. We firstly examine the underdamped regime, where[1] [1, 21]

$$\mathcal{Q}_j(t) = e^{-\Gamma_{jj}t/2}\left[Q_j \cos(\acute{\omega}_j t) + \left(\frac{P_j}{m\acute{\omega}_j} + \frac{Q_j \Gamma_{jj}}{2\acute{\omega}_j}\right)\sin(\acute{\omega}_j t)\right] \tag{18}$$

with the observed (damped) frequency of oscillation

$$\acute{\omega}_j = \sqrt{\omega_h^2 + \tilde{\omega}_j^2 - \Gamma_{jj}^2/4}. \tag{19}$$

We immediately see $\Gamma_{jj'} = 2|\tilde{\omega}_j|\delta_{jj'}$ will ensure that $\acute{\omega}_j = \omega_h$ and oscillation at the correct external frequency, a result previously suggested on the grounds of minimizing the Hamiltonian correlation time for a ring polymer in a harmonic potential, and thereby optimizing statistical sampling [23, 24]. A similar analysis to the above shows that no friction matrix in the overdamped regime will reproduce the correct oscillation frequency, as in this regime $\mathcal{Q}_j(t)$ is exponentially decaying [see Eq. (25)]. To investigate different friction strengths related to this we therefore define a parameter λ such $\Gamma_{jj'} = 2\lambda|\tilde{\omega}_j|\delta_{jj'}$.

3.2. *Spectral maximum*

The spectrum of the damped harmonic normal mode (whose Fourier transform is Eq. (18)) is given exactly by [20, 21]

$$C_{Q_jQ_j}^{\mathrm{TRPMD}}(\omega) = \frac{\Gamma_{jj}}{\beta\pi m} \frac{1}{(\omega_h^2 + \tilde{\omega}_j^2 - \omega^2)^2 + \Gamma_{jj}^2\omega^2} \tag{20}$$

such that the maximum in the spectrum will be at

$$\omega_{\max} = \sqrt{\omega_h^2 + \tilde{\omega}_j^2 - \Gamma_{jj}^2/2}, \tag{21}$$

---

[1] This expression would be equal to $Q_j(t)$ in the absence of any randomly fluctuating force.

suggesting that if the correct maximum in the position spectrum of a higher normal mode is desired, rather than the correct oscillation frequency, a friction parameter of $\lambda = 2^{-1/2}$ should be used.

However, the maximum in the momentum spectrum $C^{\mathrm{TRPMD}}_{P_jP_j}(\omega) = m^2\omega^2 C^{\mathrm{TRPMD}}_{Q_jQ_j}(\omega)$ is always at the (erroneously high) ring polymer frequency $\omega = \sqrt{\omega_h^2 + \tilde{\omega}_j^2}$ and increasing friction merely broadens the peak.

3.3. *Parabolic barrier*

For an unbound, scattering system, or where barrier dynamics are required such as thermal rate calculation, we instead consider a parabolic barrier

$$V(q) = -\tfrac{1}{2}m\omega_b^2 \tag{22}$$

and investigate whether application of friction in TRPMD will correct the qualitatively incorrect fluctuation dynamics at barriers of RPMD and CMD [30]. In Matsubara dynamics, all modes are scattering,

$$Q_j(t) = Q_j\cosh(\omega_b t) + \frac{\bar{P}_j}{m\omega_b}\sinh(\omega_b t) + i\frac{\tilde{\omega}_j}{\omega}Q_{-j}\sinh(\omega_b t) \tag{23}$$

whereas the ring polmer higher normal modes are generally bound, with a frequency of $\bar{\omega}_j = \sqrt{\tilde{\omega}_j^2 - \omega_b^2}$. As the temperature is lowered, modes become successively unbound, beginning with $j = \pm 1$ at the 'crossover' temperature [34, 39]

$$\beta_c = \frac{2\pi}{\hbar\omega_b} \tag{24}$$

and the jth normal mode will become unbound when $\beta > |j|\beta_c$, but with a scattering (imaginary) frequency of $\sqrt{\omega_b^2 - \tilde{\omega}_j^2}$.

Considering a mode which is bound in the absence of a thermostat, very weak friction ($\Gamma_{jj}^2/4 < \tilde{\omega}_j^2 - \omega_b^2$) leads to damped oscillatory motion as in Eq. (18), but with $\acute{\omega}_j = \sqrt{-\omega_b^2 + \tilde{\omega}_j^2 - \Gamma_{jj}^2/4}$. Stronger friction leads to an overdamping solution,

$$\mathcal{Q}_j(t) = e^{-\Gamma_{jj}t/2}\left[Q_j\cosh(\zeta_j t) + \left(\frac{P_j}{m\zeta_j} + \frac{Q_j\Gamma_{jj}}{2\zeta_j}\right)\sinh(\zeta_j t)\right] \tag{25}$$

where $\zeta_j = \sqrt{\omega_b^2 - \tilde{\omega}_j^2 + (\Gamma_{jj}/2)^2}$ can be considered the imaginary frequency counterpart to $\acute{\omega}_j$.

The presence of the $e^{-\Gamma_{jj}t/2}$ prefactor in Eq. (25), which in the oscillatory case of Eq. (18) causes damping but leaves the frequency untouched, means that no physical (i.e. real and positive [40]) value of the friction parameter exists which would make Eq. (25) have an unbound solution. Increasing friction merely causes the oscillator to become more overdamped.

If the normal mode is unbound in the absence of friction ($\beta > |j|\beta_c$) then Eq. (25) still holds, but the solution has a scattering component for all Γ_{jj} since $-\Gamma_{jj}/2 + \zeta_j > 0$. Addition of friction only decreases the rate of escape from the barrier (rather than increasing to ω_b) as can be observed from the vanishing escape rate at high friction,

$$\lim_{\Gamma_{jj}\to\infty} -\Gamma_{jj}/2 + \zeta_j = 2\frac{\omega_b^2 - \omega_j^2}{\Gamma_{jj}}. \tag{26}$$

In order for the largest positive unbound solution (the highest root of the characteristic equation whose solution gives Eq. (25)) to be the physical barrier frequency, the friction would have to be *negative*; $\Gamma_{jj} = -\tilde{\omega}_j^2/\omega_b$.

For the (artificial) case of a reaction whose reaction co-ordinate is solely a single non-centroid normal mode, the above result is corroborated by Kramers theory [21, 28, 41] which states that the transmission coefficient $\kappa(t)$ decreases with friction as $\lim_{t\to\infty}\kappa(t) \simeq \sqrt{1+\alpha^2} - \alpha$ where $\alpha = \Gamma_{jj}/2\bar{\omega}_j$ and $\bar{\omega}_j$ is the barrier frequency in ring-polymer space defined above. However, the transmission coefficient across a parabolic barrier is unity in Matsubara dynamics, and adding friction in TRPMD will only decrease this. Consequently, application of friction in TRPMD will not ameliorate the qualitative problems with the ring polymer higher normal modes at a barrier, and in some cases will worsen them. Nevertheless, above the crossover temperature where the dividing surface is well approximated by the (unthermostatted) centroid, this is unlikely to be of concern.

4. Numerical illustration

To illustrate some of the results of section 3 and clarify the nature of the approximations inherent in CMD, RPMD and TRPMD from Matsubara dynamics, we firstly examine the position-squared autocorrelation function for a harmonic oscillator, for which Matsubara dynamics is exactly equal to the quantum result but both RPMD and CMD fail to qualitatively reproduce [31]. CMD produces the incorrect result at $t = 0$ but then oscillates at the correct frequency (though incorrect amplitude), whereas RPMD is exact at zero time but then deviates from the quantum result at finite time due to the presence of the spurious frequencies in the higher normal modes [31, 32].

The exact quantum position-squared autocorrelation function in the harmonic potential Eq. (16) is [31, 32]

$$c_{q^2q^2}(t) = \frac{\hbar^2}{4m^2\omega_h^2}\left[\frac{2}{\beta\hbar\omega_h}\coth\left(\frac{\beta\hbar\omega_h}{2}\right)\cos(2\omega_h t) + 2\coth^2\left(\frac{\beta\hbar\omega_h}{2}\right) - 1\right]. \tag{27}$$

which in appendix B we show is exactly replicated by the Matsubara correlation function. For RPMD, it is [31, 32][1]

$$C_{q^2q^2}^{\mathrm{RPMD}}(t) = \frac{1}{\beta^2 m^2}\sum_{j=-(M-1)/2}^{(M-1)/2}\frac{1}{\omega_h^2+\tilde{\omega}_j^2}\left\{\frac{2\cos^2[(\omega_h^2+\tilde{\omega}_j^2)^{1/2}t]}{\omega_h^2+\tilde{\omega}_j^2} + \sum_{k=-(M-1)/2}^{(M-1)/2}\frac{1}{\omega_h^2+\tilde{\omega}_k^2}\right\} \tag{28}$$

---

[1] The RPMD and TRPMD correlation functions given here use the Matsubara frequencies $\tilde{\omega}_j$, and converge to the conventional form using the ring-polymer frequencies in the large M and large N limit. The numerical results use the ring-polymer frequencies with $N = 501$, and their convergence with the same correlation function computed with Matsubara frequencies ($M = 501$) was checked.

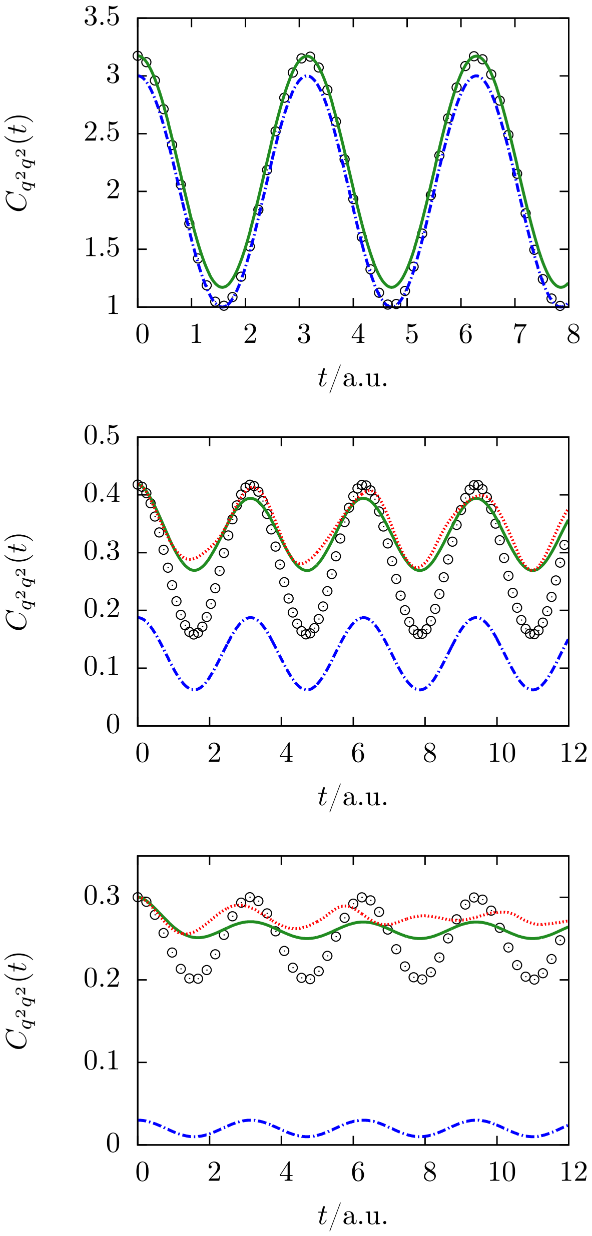

Figure 1. Position-squared autocorrelation function for a harmonic oscillator, with $\beta = 1$ (top), $\beta = 4$ (middle) and $\beta = 10$ (bottom). Black circles, quantum; solid green line, TRPMD (with optimal damping); red dots, RPMD; blue dot-dashes, CMD. At $\beta = 1$ the TRPMD and RPMD lines are identical to within graphical accuracy and only the former is shown.

whereas the TRPMD result for $\lambda = 1$ ($\Gamma_{jj'} = 2|\tilde{\omega}_j|\delta_{jj'}$) is

$$
\begin{aligned}
C_{q^2q^2}^{\mathrm{TRPMD}}(t) = & \frac{1}{\beta^2 m^2} \sum_{j=-(M-1)/2}^{(M-1)/2} \frac{1}{\omega_h^2 + \tilde{\omega}_j^2} \left\{ \frac{2e^{-2|\tilde{\omega}_j|t}}{\omega_h^2 + \tilde{\omega}_j^2} \left[\cos(\omega_h t) + \frac{\tilde{\omega}_j}{\omega_h} \sin(\omega_h t) \right]^2 \right. \\
& \left. + \sum_{k=-(M-1)/2}^{(M-1)/2} \frac{1}{\omega_h^2 + \tilde{\omega}_k^2} \right\}. \qquad (29)
\end{aligned}
$$

For comparison, the CMD position-squared autocorrelation function (using the

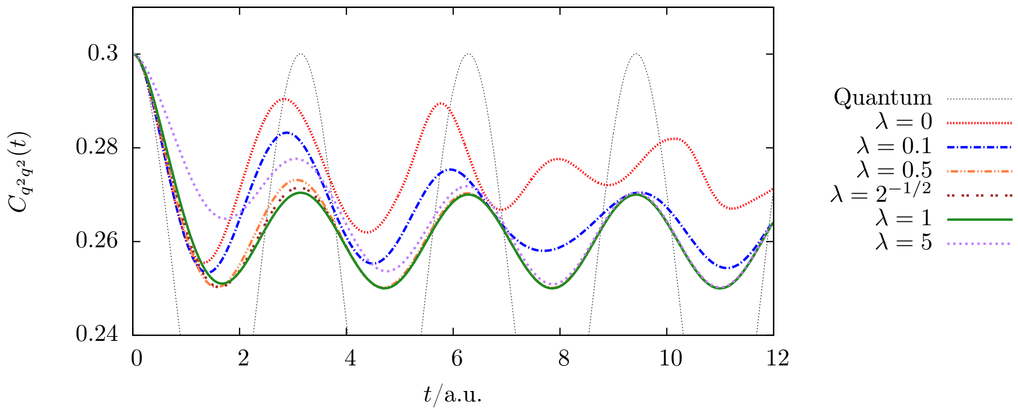

Figure 2. Position-squared autocorrelation function for a harmonic oscillator at $\beta = 10$, showing the exact quantum result and TRPMD at a varying friction parameters. For clarity, the figure is zoomed in around the TRPMD correlation function.

CMD with classical operators method [14, 15, 24, 31][1]) is

$$C^{\mathrm{CMD}}_{q^2q^2}(t) = \frac{1}{(\beta m\omega_h^2)^2}\left[2\cos(\omega_h t)^2 + 1\right]. \tag{30}$$

We use parameters to facilitate comparison with previous literature [31]; $\hbar = k_{\mathrm{B}} = m = \omega_h = 1$ and results for systems of varying β are presented in Fig. 1.

At high temperatures ($\beta = 1$), all methods are a good approximation to the quantum result and the RPMD and TRPMD results are indistinguishable to within graphical accuracy (such that only the TRPMD result is plotted). At $\beta = 4$, the amplitude of oscillations is incorrect for all methods, though TRPMD starts at the correct value whereas CMD is too low. The RPMD correlation function shows deviations from harmonic behaviour due to the higher normal modes. At $\beta = 10$, the CMD correlation function is incorrect at zero time and RPMD cannot replicate the oscillations, whereas TRPMD captures both properties.

We then examine the effect of different friction parameters in Fig. 2, choosing the $\beta = 10$ system to exemplify the effect of damping. Regardless of λ, all TRPMD correlation functions have the correct zero-time value. The $\lambda = 0$ (RPMD) result oscillates erratically, as in the third panel of Fig. 1. Applying very small friction ($\lambda = 0.1$) noticeably improves the correlation function but contamination from higher normal modes is still evident. In accordance with Eq. (19), $\lambda = 1$ has exactly the correct oscillation frequcency, though for $0.5 \leq \lambda \leq 1$ the correlation functions are very similar, settling to the correct frequency (though incorrect amplitude) after one oscillation. Increasing the friction yet further ($\lambda = 5$) causes the correct oscillation frequency (as all modes apart from the centroid are overdamped) but the slow decay of the heavily overdamped higher normal modes causes the midpoint of the oscillation to decay slowly over time.

To illustrate the results of section 3.2 we then plot the position spectrum in Fig. 3 for the first normal mode $j = 1$ at $\beta = 10$, showing how increasing friction causes the TRPMD peak to redshift and broaden from the $\lambda = 0$ (RPMD) peak at $\omega = \sqrt{1 + (\pi/5)^2} \simeq 1.18$ to the (external) value of $\omega = 1$ at $\lambda = 2^{-1/2}$ and onto a peak centred on $\omega = 0$ at $\lambda = 5$. The same is seen for other values of β and j

---

[1] We note that there are many other approaches of varying mathematical complexity and accuracy for the computation of general correlation functions with CMD[9–12, 14, 16, 31], and here restrict ourselves to methods which simply require direct computation of a correlation function.

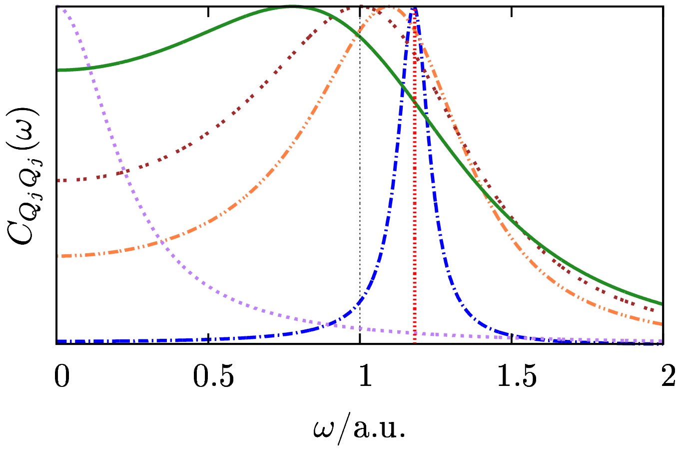

Figure 3. Position spectrum of the first normal mode ($|j| = 1$) of a harmonic oscillator at $\beta = 10$ for the same set of friction parameters (with the same line styles) as in Fig. 2. To aid comparison, the intensities for different λ are normalized such that their maxima are equal.

Observable	Suggested friction parameters (λ)	
	Numerical results	Harmonic analysis
Oscillation frequency, $C_{q^2q^2}(t)$	–	1
Spectral peaks	$\simeq 0.5$	$2^{-1/2}$
Rate calculation	generally 0	0

Table 1. Comparison of friction parameters suggested by previous numerical studies [24, 28] and the present harmonic analysis. $\lambda = 0$ is equivalent to RPMD.

(results not shown), with the redshifting and broadening more pronounced as β decreases and j rises.

5. Discussion

The optimal friction parameters suggested by the present work are compared with those of previous numerical studies in Table 1. Although the value of $\lambda = 2^{-1/2}$ (for correct spectral maxima) suggested here is slightly larger than the value of $\lambda = 0.5$ suggested by a previous numerical study [24], that study also found that broadly similar numerical results were obtained for a wide range of parameters around $\lambda = 0.5$. We also note that Ref. [24] computed the spectrum of the overall ring polymer (generally modelled as its centroid [26]) rather than the spectrum of a single normal mode, so the effect of friction is seen indirectly via coupling between the centroid and higher normal modes through anharmonicity in the potential.

We suspect that a numerically favourable value of $\lambda = 1/2$ is due to interplay between shifting the frequencies of the higher normal modes to the external frequency (implying $\lambda = 1$), moving the maximum in the spectral peak (implying $\lambda = 2^{-1/2}$), and avoiding harsh damping which would decorrelate the modes too quickly to capture their dynamics and broaden spectral peaks [25] (implying the weakest possible friction which removes spurious resonances).

The result that zero friction (i.e. RPMD) is most accurate for rate calculation is broadly supported by a previous numerical study [28].

The friction matrix $\Gamma_{jj'} = 2\lambda|\tilde{\omega}_j|\delta_{jj'}$ obtained in section 3.1 corresponds to critical damping of the ring polymer springs in the absence of an external potential for $\lambda = 1$ [23, 24], but not critical damping of the ring polymer modes in a harmonic oscillator (where the external frequency must also be considered), and can be determined without knowledge of the frequencies present in the external potential.

	CMD	RPMD	TRPMD
Approximation	Mean field	Discard $i\mathcal{L}_{\Im}^{[M]}$	Replace $i\mathcal{L}_{\Im}^{[M]}$ with $\mathcal{A}_{\mathrm{wn}}^{[M]\dagger}$
Force on centroid	Mean-field Matsubara force	Exact Matsubara force	Exact Matsubara force
Rate calculation	Good while centroid optimal dividing surface	Good approximation despite incorrect fluctuations	Friction decreases rates
Spectra	Curvature problem as mean field neglects fluctuations	Resonance problem as incorrect frequencies	Good approximation as correct frequencies or spectral peak
Nonlinear operators	Fails as non-centroid modes undefined	Breaks down faster than linear due to incorrect frequencies	Breaks down faster than linear due to damping
Advised usage	Rates above crossover	Rates, diffusion	Spectra

Table 2. Summary of properties of CMD, RPMD and TRPMD obtained from their approximations to Matsubara dynamics and their advised usage. Some of columns 2 and 3 adapted from Ref. [30]. See text.

Obviously, chemical systems will not be purely harmonic but in many systems (such as vibrating bond) this will be a reasonable approximation.

This definition of the friction matrix means that the centroid is unthermostatted for all λ, so the results which have previously been derived for TRPMD for an arbitrary friction matrix which does not thermostat the centroid, such as its short-time error compared to the quantum result [24] and detailed balance [28], still hold. A new result is that TRPMD, like RPMD, will have the exact Matsubara force on the centroid, since the error term does not act upon the centroid. Furthermore, the error scaling in the higher normal modes in time will be the same as that for RPMD, namely $i\mathcal{L}_{\Im}^{[M]} - \mathcal{A}_{\mathrm{wn}}^{[M]\dagger} \propto 1/\beta\hbar$.

This choice of friction matrix means that the TRPMD correlation function of a linear operator will deviate from the Matsubara correlation function due to higher-order coupling between the centroid dynamics and the damping (and random kicks) of the higher normal modes via anharmonicity in the potential. This explains the numerically observed slight broadening of spectral lines (a far smaller issue than the curvature problem of CMD or the spurious resonances of RPMD) [24], and the slower reaction rates beneath the crossover temperature [28]. For nonlinear operators, TRPMD (like RPMD) would be expected to break down faster than for linear operators due to the error term only acting directly on the higher normal modes, though the example of the position-squared autocorrelation function given above suggests that with a careful choice of friction the breakdown may not be too drastic.

All the results presented here generalize immediately to multidimensional systems, where the friction is applied in $F(N-1)$ normal modes and springs exist between N replicas of the physical system. For nonlinear operators one cannot, in general, easily relate the Kubo and Generalized Kubo forms (the position-squared operator explored above being an exception). For reaction rates involving the highly nonlinear flux and side operators this is partially resolved by relating the generalized Kubo form to the exact quantum expression when there is no recrossing of the path-integral dividing surface (and those orthogonal to it in path-integral space) [39, 42–44].

6. Conclusions

In this article we have given the error term between thermostatted ring polymer molecular dynamics (TRPMD) and Matsubara dynamics, the examination of which shows that TRPMD has some (previously unknown) favourable properties, such that the force on the centroid is the exact Matsubara force, and that for a harmonic well, TRPMD can replicate either the correct oscillation frequency or the spectral maximum, depending on the applied friction, and improve upon both RPMD and CMD for computation of the position-squared autocorrelation function. The results are broadly consistent with previously known properties of TRPMD (such as conservation of the quantum Boltzmann distribution) and previous numerical studies [24, 25, 28], with a harmonic analysis explaining the success of TRPMD for spectral calculation and lacklustre performance in rate calculation.

By examining when the approximations made in constructing CMD, RPMD and TRPMD are likely to be valid or not, as is sketched in Table 2, one can make *a priori* suggestions of when each method is likely to be accurate and advise their usage. Of course, this does not guarantee accuracy but would suggest the method which is most likely to work for a given system. Although some of the results are derived in the harmonic limit, we would also expect them to hold in physically realistic systems which are moderately harmonic, and for highly anharmonic or pathological systems further analysis would be required.

It could be that a generalized Langevin equation [21, 23, 45] may be more successful than a simple white noise thermostat for spectral calculation[1], as might usage of unphysical negative friction for reaction rates [40, 46]. Future research could also include extension to non-adiabatic systems where RPMD has been successful [47–54].

In closing, the results obtained in this paper place TRPMD on a firmer theoretical footing by relating it to Matsbara dynamics (and thereby to the exact quantum result), and give insights into the preferable friction parameter. They advise the use of TRPMD for the computation of spectra and other properties of bound systems where the correct oscillation frequencies or spectral peaks are required, and caution against usage for rate calculation beneath the crossover temperature.

Appendix A. Analyticity in the complex plane

Here we show that the complex dynamics generated by $\mathcal{L}_{\bar{\mathbf{P}}}^{[M]}$ is analytic everywhere in the complex plane of $\mathbf{P}$, such that Eq. (1) is equal to Eq. (11). Consider an observable $B(\mathbf{P}, \mathbf{Q}, t)$, which is propagated by the Liouvillian

$$\mathcal{L} = (\nabla_{\mathbf{P}} H) \cdot \nabla_{\mathbf{Q}} - (\nabla_{\mathbf{Q}} H) \cdot \nabla_{\mathbf{P}} \tag{A1}$$

where H is the Hamiltonian of the system and an analytic, but not necessarily real, function of $\mathbf{P}$ and $\mathbf{Q}$. The propagation is formally

$$\frac{d}{dt} B(\mathbf{P}, \mathbf{Q}, t) = \mathcal{L} B(\mathbf{P}, \mathbf{Q}, t) \tag{A2}$$

$$B(\mathbf{P}, \mathbf{Q}, t) = e^{\mathcal{L} t} B(\mathbf{P}, \mathbf{Q}, 0) \tag{A3}$$

This (obviously) requires $B(\mathbf{P}, \mathbf{Q}, t)$ to be single valued, and the exponentiated expression Eq. (A3) to exist. If $B(\mathbf{P}, \mathbf{Q}, t)$ is an analytic function for all values of

---

[1] Michele Ceriotti, private communication, 2015.

$\mathbf{P}$ and $\mathbf{Q}$, then (by the Cauchy-Riemann relations)

$$\frac{\partial}{\partial P_j^*} B(\mathbf{P}, \mathbf{Q}, t) = 0 \ \forall j \tag{A4}$$

where P_j^* is the complex conjugate of P_j (and likewise for Q_j^*). If H is analytic then

$$\frac{\partial}{\partial P_j^*} H = 0 \ \forall j \tag{A5}$$

which means that (using H being continuous, Schwarz' theorem and therefore $\frac{\partial}{\partial P_j^*}\frac{\partial}{\partial P_j} = \frac{\partial}{\partial P_j}\frac{\partial}{\partial P_j^*}$) the commutation relations exist

$$\frac{\partial}{\partial P_j^*}\mathcal{L} = \mathcal{L}\frac{\partial}{\partial P_j^*}. \tag{A6}$$

Using the definition of an exponential as its power expansion we then see,

$$\begin{aligned}
\frac{\partial}{\partial P_j^*} B(\mathbf{P}, \mathbf{Q}, t) =& \frac{\partial}{\partial P_j^*} e^{\mathcal{L}t} B(\mathbf{P}, \mathbf{Q}, 0) && \text{(A7)} \\
=& e^{\mathcal{L}t} \frac{\partial}{\partial P_j^*} B(\mathbf{P}, \mathbf{Q}, 0) && \text{(A8)} \\
=& 0 && \text{(A9)}
\end{aligned}$$

so $B(\mathbf{P}, \mathbf{Q}, t)$ remains an analytic function of P_j for all time (and likewise for Q_j). This is true $\forall j$ (and $\forall t$), and by Hartog's Theorem, true for $B(\mathbf{P}, \mathbf{Q}, t)$ everywhere. This means that $B(\mathbf{P}, \mathbf{Q}, t)$ obeys the Cauchy Riemann relations and can have no poles in the complex plane. The Boltzmann distribution is also holomorphic, and provided that the zero-time observable $A(\mathbf{P}, \mathbf{Q}, 0)$ is also holomorphic (which almost all physical observables are) the entire integrand of Eq. (1) will be.

We then complete the square in the complex Matsubara distribution, giving Eq. (11) where the edges of the rectangle used in the contour integration are

$$\begin{aligned}
\mathcal{E}(t) = & \lim_{\boldsymbol{\pi}\to\infty} \frac{\alpha_M}{2\pi\hbar} \int d\mathbf{Q} \left[\prod_{j=-(M-1)/2}^{(M-1)/2} i \int_0^{m\omega_j Q_{-j}} d\Pi_j \right] \\
& \times e^{-\beta[H(\boldsymbol{\pi}+i\boldsymbol{\Pi},\mathbf{Q})-i\theta(\boldsymbol{\pi}+i\boldsymbol{\Pi},\mathbf{Q})]} A(\mathbf{Q}) e^{\mathcal{L}^{[M]}_{\boldsymbol{\pi}+i\boldsymbol{\Pi}}t} B(\mathbf{Q}) \\
& + \lim_{\boldsymbol{\pi}\to-\infty} \frac{\alpha_M}{2\pi\hbar} \int d\mathbf{Q} \left[\prod_{j=-(M-1)/2}^{(M-1)/2} i \int_0^{m\omega_j Q_{-j}} d\Pi_j \right] \\
& \times e^{-\beta[H(\boldsymbol{\pi}+i\boldsymbol{\Pi},\mathbf{Q})-i\theta(\boldsymbol{\pi}+i\boldsymbol{\Pi},\mathbf{Q})]} A(\mathbf{Q}) e^{\mathcal{L}^{[M]}_{\boldsymbol{\pi}+i\boldsymbol{\Pi}}t} B(\mathbf{Q})
\end{aligned} \tag{A10}$$

where $\pi_j = \Re P_j$, $\Pi_j = \Im P_j$, and $\mathcal{L}^{[M]}_{\boldsymbol{\pi}+i\boldsymbol{\Pi}}$ is the Matsubara Liouvillian Eq. (4) continued into the complex plane.

The edge terms can be proven to be zero in a number of limits. Specifically, for $A(\mathbf{Q})$ and $B(\mathbf{Q})$ which are at most exponential in $\mathbf{P}$ and/or $\mathbf{Q}$, the edge terms will vanish when the trajectories are real ($\boldsymbol{\Pi} = 0$) where conservation of energy arguments can be used in a bound system and in a scattering system whose potential tends to a constant value far out. The edges will also be zero in any system at $t = 0$ where the momentum integral can be evaluated analytically, and where discarding $\mathcal{L}_{\Im}^{[M]}$ (and thereby keeping the trajectories real) is no approximation, namely up to $\mathcal{O}(t^2)$ for nonlinear operators and $O(t^6)$ for linear operators [24, 30].

For systems where the trajectories are known analytically, such as a free particle, parabolic well and barrier, even though $\boldsymbol{\pi}(t) \to \infty$ as $\boldsymbol{\pi}(0) \to \infty$, careful consideration of the limits and application of l'Hôpital's rule shows that the edge term still vanishes.

Despite the above promising results, trajectories in the complex plane are frequently not bounded [36] and in general it is difficult to determine whether or not terms of the form in Eq. (A10) will converge [37] for any general potential. A proof of whether $\mathcal{E}(t)$ can be neglected in any general case is left as further work.

Appendix B. Equivalence of quantum and Matsubara position-squared autocorrelation functions

To show that the Matsubara correlation function is equivalent to Eq. (27), we firstly calculate the Matsubara correlation function using the harmonic analysis in the supplementary material of Ref. [30], giving

$$\begin{aligned} C_{q^2q^2}^{[N]}(t) =& \frac{1}{\beta^2 m^2 \omega_h^4}\Bigg[\cos(2\omega_h t)\sum_{j=-(M-1)/2}^{(M-1)/2}\frac{1}{1+(\tilde{\omega}_j/\omega_h)^2} + \sum_{j=-(M-1)/2}^{(M-1)/2}\frac{1-(\tilde{\omega}_j/\omega_h)^2}{(1+(\tilde{\omega}_j^2/\omega_h))^2} \\ &+ \sum_{j=-(M-1)/2}^{(M-1)/2}\sum_{k=-(M-1)/2}^{(M-1)/2}\frac{1}{1+(\tilde{\omega}_j/\omega_h)^2}\frac{1}{1+(\tilde{\omega}_k/\omega_h)^2}\Bigg] \end{aligned} \tag{B1}$$

The Matsubara frequency summation [55] is performed by examining the integral

$$\oint dz \frac{\cot(z)}{z^2 + x^2} \tag{B2}$$

around a circle of infinite radius, origin zero, giving

$$x\coth(x) = \lim_{M\to\infty}\sum_{j=-(M-1)/2}^{(M-1)/2}\frac{1}{1+(j\pi/x)^2} \tag{B3}$$

and by differentiation of Eq. (B3), that

$$x^2[\coth^2(x) - 1] = \lim_{M\to\infty}\sum_{j=-(M-1)/2}^{(M-1)/2}\frac{1-(j\pi/x)^2}{(1+(j\pi/x)^2)^2}. \tag{B4}$$

Subsituting $x = \beta\hbar\omega_h/2$ into Eq. (B3) and Eq. (B4), and these expressions into Eq. (B1) gives Eq. (27) as required.

Acknowledgements

This work was supported by a Research Fellowship from Jesus College, Cambridge. The author wishes to thank Stuart Patching for suggesting the contour integral in

Eq. (B2), and is also grateful for corrections to and comments on the manuscript from Michael Willatt, advice from Stuart Althorpe and Michele Ceriotti, and for helpful discussions with Robert Whelan and Adam Harper.

References

[1] C. Gardiner, *Stochastic Methods* (Springer, Berlin, 2009).
[2] R. Zwanzig, *Nonequilibrium statistical mechanics* (Oxford University Press, New York, 2001).
[3] S. Habershon, D.E. Manolopoulos, T.E. Markland and T.F. Miller, Annu. Rev. Phys. Chem. **64** (1), 387 (2013).
[4] J. Liu, Int. J. Quantum Chem., DOI 10.1002/qua.24872 (2015).
[5] W.H. Miller, PNAS **102** (19), 6660 (2005).
[6] E. Wigner, Phys. Rev. **40**, 749 (1932).
[7] J. Liu and W.H. Miller, J. Chem. Phys. **126** (23), 234110 (2007).
[8] Q. Shi and E. Geva, J. Chem. Phys. **118** (18), 8173 (2003).
[9] J. Cao and G.A. Voth, J. Chem. Phys. **100** (7), 5093 (1994).
[10] J. Cao and G.A. Voth, J. Chem. Phys. **100** (7), 5106 (1994).
[11] J. Cao and G.A. Voth, J. Chem. Phys. **101** (7), 6157 (1994).
[12] J. Cao and G.A. Voth, J. Chem. Phys. **101** (7), 6168 (1994).
[13] J. Cao and G.A. Voth, J. Chem. Phys. **101** (7), 6184 (1994).
[14] G.A. Voth, *Path-Integral Centroid Methods in Quantum Statistical Mechanics and Dynamics* Adv. Chem. Phys. (1996), pp. 135–218.
[15] K. Kinugawa, Chemical Physics Letters **292** (4-6), 454 (1998).
[16] D.R. Reichman, P.N. Roy, S. Jang and G.A. Voth, J. Chem. Phys. **113** (3), 919 (2000).
[17] I.R. Craig and D.E. Manolopoulos, J. Chem. Phys. **121** (8), 3368 (2004).
[18] I.R. Craig and D.E. Manolopoulos, J. Chem. Phys. **122** (8), 084106 (2005).
[19] I.R. Craig and D.E. Manolopoulos, J. Chem. Phys. **123** (3), 034102 (2005).
[20] M. Ceriotti, Ph.D. thesis, ETH Zürich 2010.
[21] A. Nitzan, *Chemical Dynamics in Condensed Phases* (Oxford University Press, New York, 2006).
[22] G. Bussi and M. Parrinello, Phys. Rev. E **75**, 056707 (2007).
[23] M. Ceriotti, M. Parrinello, T.E. Markland and D.E. Manolopoulos, J. Chem. Phys. **133** (12), 124104 (2010).
[24] M. Rossi, M. Ceriotti and D.E. Manolopoulos, J. Chem. Phys. **140** (23), 234116 (2014).
[25] M. Rossi, H. Liu, F. Paesani, J. Bowman and M. Ceriotti, J. Chem. Phys. **141** (18), 181101 (2014).
[26] A. Witt, S.D. Ivanov, M. Shiga, H. Forbert and D. Marx, J. Chem. Phys. **130** (19), 194510 (2009).
[27] S.D. Ivanov, A. Witt, M. Shiga and D. Marx, J. Chem. Phys. **132** (3), 031101 (2010).
[28] T.J.H. Hele and Y.V. Suleimanov, J. Chem. Phys. **143** 074107 (2015).
[29] T.J.H. Hele, M.J. Willatt, A. Muolo and S.C. Althorpe, J. Chem. Phys. **142** (13), 134103 (2015).
[30] T.J.H. Hele, M.J. Willatt, A. Muolo and S.C. Althorpe, J. Chem. Phys. **142** (19), 191101 (2015).
[31] A. Horikoshi and K. Kinugawa, J. Chem. Phys. **122** (17), 174104 (2005).
[32] S. Jang, A.V. Sinitskiy and G.A. Voth, J. Chem. Phys. **140** (15), 154103 (2014).
[33] R. Kubo, J. Phys. Soc. Jpn. **12** (6), 570 (1957).
[34] J.O. Richardson and S.C. Althorpe, J. Chem. Phys. **131** (21), 214106 (2009).
[35] T. Matsubara, Progress of Theoretical Physics **14** (4), 351 (1955).
[36] C.M. Bender, D.C. Brody and D.W. Hook, Journal of Physics A: Mathematical and Theoretical **41** (35), 352003 (2008).
[37] G. Aarts, E. Seiler and I.O. Stamatescu, Phys. Rev. D **81**, 054508 (2010).
[38] T.D. Hone, P.J. Rossky and G.A. Voth, J. Chem. Phys. **124** (15), 154103 (2006).
[39] T.J.H. Hele and S.C. Althorpe, J. Chem. Phys. **138** (8), 084108 (2013).
[40] J. MacFadyen, J. Wereszczynski and I. Andricioaei, J. Chem. Phys. **128** (11), 114112 (2008).
[41] H. Kramers, Physica **7** (4), 284 (1940).
[42] S.C. Althorpe and T.J.H. Hele, J. Chem. Phys. **139** (8), 084115 (2013).
[43] T.J.H. Hele and S.C. Althorpe, J. Chem. Phys. **139** (8), 084116 (2013).
[44] T.J.H. Hele, Quantum Transition-State Theory, PhD Thesis, University of Cambridge, 2014.

[45] M. Ceriotti, G. Bussi and M. Parrinello, Journal of Chemical Theory and Computation **6** (4), 1170 (2010).

[46] L.Y. Chen, S.C. Ying and T. Ala-Nissila, Phys. Rev. E **65**, 042101 (2002).

[47] T.J.H. Hele, An electronically non-adiabatic generalization of ring polymer molecular dynamics, Master's thesis, Exeter College, University of Oxford, 2011.

[48] N. Ananth, J. Chem. Phys. **139** (12), 124102 (2013).

[49] N. Ananth and T.F. Miller, J. Chem. Phys. **133** (23), 234103 (2010).

[50] A.R. Menzeleev, F. Bell and T.F. Miller, J. Chem. Phys. **140** (6), 064103 (2014).

[51] J.O. Richardson and M. Thoss, J. Chem. Phys. **139** (3), 031102 (2013).

[52] J.O. Richardson and M. Thoss, J. Chem. Phys. **141** (7), 074106 (2014).

[53] A.R. Menzeleev, N. Ananth and T.F. Miller III, J. Chem. Phys. **135** (7), 074106 (2011).

[54] J.S. Kretchmer and T.F. Miller III, J. Chem. Phys. **138** (13), 134109 (2013).

[55] A. Altland and B. Simons, *Condensed matter field theory* (Cambridge University Press, New York, 2010; pp. 168–171), pp. 168–171.